Available online at www.sciencedirect.com

ScienceDirect

Energy Procedia 49 (2014) 428 – 437

Energy Procedia

SolarPACES 2013

Numerical simulation on the performance of a combination of external and cavity absorber for solar power plant

Y Luo, XZ Du*, LJ Yang, YP Yang

Key Laboratory of Condition Monitoring and Control for Power Plant Equipment of Ministry of Education, North China Electric Power University, Beijing 102206, China

Abstract

Optical and thermal simulation of a new up-down arranged dual-receiver for solar tower plant is presented in this paper. The top receiver is an external absorber type to serve as the boiling section, the bottom receiver is a cavity type to serve as the superheating section. The heliostat field is divided into two parts respectively for boiling and superheating section, it is quick and simple to control the heat flux distribution on both section. Then multi-aiming strategy is used for avoiding appearance of heat spot. For cavity receiver, a optimized layout for tubes is to increase convective heat transfer coefficient in the high heat flux religions. The concept of this new receiver is illustrated by a 10 MW_e solar power plant that produces main steam at 513.5 $°C$ and pressure of 10.12 MPa. Finally, this dual-receiver has a thermal efficiency of 91 %.

Selection and peer review by the scientific conference committee of SolarPACES 2013 under responsibility of PSE AG.
Final manuscript published as received without editorial corrections.
Keywords: Solar tower; Dual-receiver; Heat transfer

1. Introduction

Among the solar thermal tower plants that have been built and used water as heat transfer fluid, Solar One, as an external absorber type, its superheating section operates in the once-through mode and the start-up strategy of the system is complex. CESA- I, as a single cavity type, a drum separates its boiling and superheating section. However, as both sections are placed in a singe cavity, the aiming strategy of the heliostat field is complex and it is

* Corresponding author. Tel.: +86-105-197-1326;
E-mail address: duxz@ncepu.edu.cn

Selection and peer review by the scientific conference committee of SolarPACES 2013 under responsibility of PSE AG.
Final manuscript published as received without editorial corrections.
doi:10.1016/j.egypro.2014.03.046

not easy to control and get accurate heat flux distribution for boiling and superheating section. Therefore, the start-up time is still long. PS10 [1] and PS20 just heat water to saturated steam. Therefore, the arrangement of boiling and superheating sections in the receiver plays an important role in the operation of the solar thermal tower plants.

Recent years some researches have been done on separation of boiling and superheating. A patent is published which comprises two cavities laid up and down to separately apply for the boiling and superheater subsystem [2]. In this way, heliostats layout is limited by the aperture of cavity. Heliostats have to be placed further for high capacity power plant such as 50 MW_e and it will decrease total heliostat field efficiency. Another configuration reported recently is a integrated receiver that has a boiling section in tandem with a superheating section. The receiver has a north-centered opening sector of 72°. The inner is 14 m in diameter made of 1318 tubes acted as superheater. The outer is of 16 m diameter made of 1506 tubes acted as boiler [3]. As two sections are so close to each other, radiation spillage and conduction between them makes it not easy to control and calculate final heat flux distribution.

A new configuration proposed in this work is a combination of external and cavity absorber for solar tower plant. It is a dual-receiver which places an external absorber at the height of 103 m and a cavity absorber at 91.5 m high, as can be seen in Fig. 2. The top receiver serves as the boiling section so that the solar power plants can have a larger scale with a surrounding heliostat field. And the boiling temperature is relatively low, leading to small convection and radiation heat losses. The bottom receiver serves as the superheating section. Considering the superheating temperature exceeds 500 $°C$, cavity structure can reduce the convection and radiation losses. Finally, a steam drum is arranged on the top of the boiling receiver. The final goal is to create a 10 MW_e solar thermal power plant of dual-receiver type that its main steam temperature is at 513.5 $°C$ and pressure of 10.12 MPa.

2. Heliostat field design

The target of the heliostat field is to meet a 10 MW_e solar thermal power plant of dual-receiver type. It makes the duel-receiver collect about 57 MW_{th} at the design point of equinox noon, latitude 40.4° North, DNI=900 W/m^2. Among the total heat absorption, 25 % amount of it is stored and supplies heat at the night. The locating method of heliostat field is a simple preliminary design to ensure no blocking loss over the year and efficient use of land [4] when assuming total solar receiver is at the height of 103 m.

The field boundary efficiency defines as product of cosine efficiency and atmospheric attenuation efficiency to determine the most efficient heliostats. Even though the total solar field efficiency also includes spillage, shading and blocking efficiency. Spillage loss is relatively low for small-scale heliostat field. Shading and blocking loss has less influence on the total efficiency than other losses for choosing a heliostat filed layout of no blocking loss over the year. As shown in Fig. 3, the heliostat field is divided into two parts: the red one consists of 704 heliostats corresponding to the top external boiling receiver limited by the field boundary efficiency of 0.669, the yellow one has 188 heliostats corresponding to the bottom cavity superheating receiver confined to field boundary efficiency of 0.908.

Each heliostat has a 10 m by 10 m surface with reflectivity of 0.9. The centre of heliostat is at the height of 5.2 m. Then the position of every heliostat is put into the ray-tracing model SolTrace [5] to get the final heat flux distribution on the dual-receiver. Multi-aiming focusing strategy is applied to get uniform and not large spot. As SolTrace does not support atmospheric attenuation loss calculation, average atmospheric attenuation efficiency value is calculated by program and converted into reflectivity. Mirror errors, tracking errors and sun shape errors are respectively 2 mrad, 1 mrad and 2.51 mrad assuming Gaussian distribution. The combination of mirror and tracking errors is converted into specularity errors in the SolTrace software. And The total heliostat field efficiency is 70.4%.

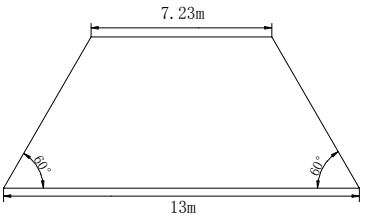

Fig. 1. Top view of the cavity receiver.

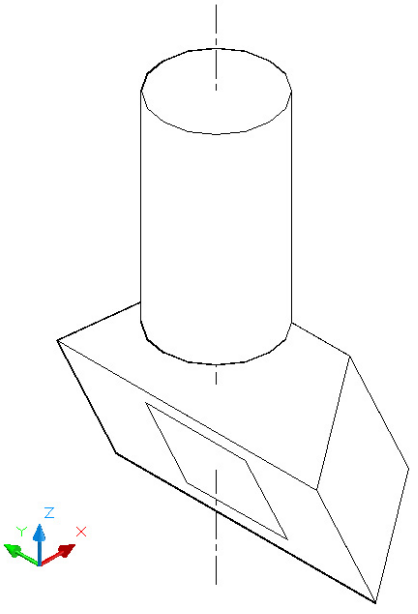

Fig. 2. Geometry of dual-receiver.

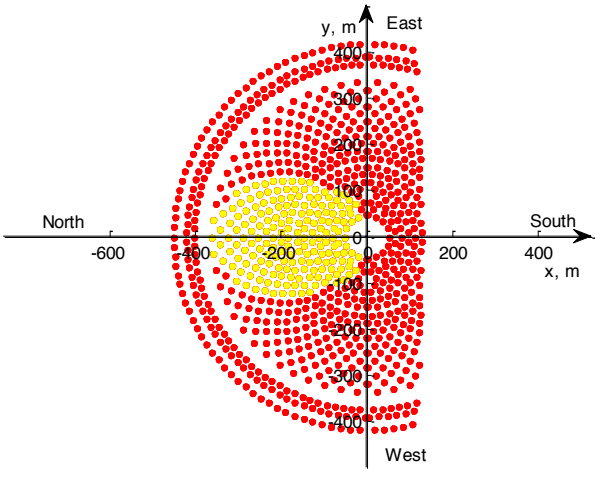

Fig. 3. Heliostat field layout.

3. Numerical simulation of the solar receiver

3.1. Dual-receiver dimensions

The up-down arranged dual-receiver for solar thermal power plant is shown in Fig. 2. The top external receiver locates at 103 m and has cylinder shape with length of 10 m and diameter of 5.3 m. The receiver comprises 18 parallel panels, each panel has 15 tubes. The inner diameter of tube is 26 mm, the outer is 32 mm. Tube spacing is 32 mm. And assuming that tubes with spacing between them have no effect on the reflective losses and will not decrease the efficiency of the receiver. The boiler is of a drum type with forced circulation.

The bottom receiver locates at 91.5 m and has configuration of trapezoidal cavity of 7 m high. The receiver inclination is 25 ° and has a 5 m by 5 m aperture. The centre of cavity aperture and cylinder are in a vertical line. The top view of cavity can be seen in Fig. 1. The inner side two walls each has 2 panels, each panel has 35 tubes. The back wall has totally 6 panels and 22 tubes of every panel. The outer tube diameter is 24 mm with thickness of 2 mm. Tube spacing is as 2.5 times as the outer diameter. The material of all tubes is austenitic stainless steel with heat conductivity coefficient of about 20 W/(m·k). And the gap between up and down receiver is filled with concrete.

3.2. Multi-aiming strategy

To get more uniform heat flux distribution and avoid the appearance of hot spot, a multi-aiming strategy is presented in this part. For the boiling receiver, it comprises of five radial groups. The aiming points of these groups are up and down, back and front derived from the centre of cylinder. And solar rays from the heliostats are intercepted by the boiler tubes before they reach the focal points. The focal points corresponding to each group in the global coordinate is described as:

$$x_B = \begin{cases} -1.1m & x_H \le 0m \\ 1.1m & x_H > 0m \end{cases} \tag{1}$$

$$z_B = \begin{cases} 101.7m & \mathrm{R} \le 90m, \mathrm{y}_B = 0m \\ 102.1m & 90m < R \le 220m, \mathrm{y}_B = 0m \\ 103m & 220m < R \le 330m, \mathrm{y}_B = 0m \\ 105m & 330m < R \le 400m, \mathrm{y}_B = 0m \\ 105.5m & \mathrm{R} > 400m, \mathrm{y}_B = 0m \end{cases} \tag{2}$$

where R is the distance from the heliostat to the tower, x_B , y_B , z_B are coordinates of the aiming points for boiling section. x_H is heliostat coordinate.

The final incident heat flux distribution for boiling receiver given by SolTrace software is shown in Fig. 4. The front half cylinder facing north has higher heat flux than the back half one. The reasons are that heliostats in the north part are more efficient than those in the south and more heliostats are placed in the north.

For heliostats supplied for the superheating receiver, it is divided into three parts. Three up-down offset aiming points lay on the entrance of cavity. One is put in the centre of aperture, the remaining two respectively lay 0.5 m up offset and 1 m down offset the centre in the coordinate of cavity. Considering inclination of cavity, layout for the focal points in the global coordinate is presented as:

$$z_S = \begin{cases} 91.95m & R \le 210m\ , y_S = 0m\ , x_S = -0.2113m \\ 91.5m & 210 < R \le 230m\ , y_S = 0m\ , x_S = 0m \\ 90.6m & R > 230m\ , \mathrm{y}_S = 0m, x_S = 0.4226m \end{cases} \tag{3}$$

where x_s, y_s, z_s are coordinates of the aiming points for superheating section.

Incident heat flux distribution on the cavity inner walls is shown in Fig. 5. It can be seen that along height heat flux is comparatively uniform.

3.3. Heat transfer in the solar receiver

Boiling receiver collects about 42 MW_{th} and superheating receiver gets 14.5 MW_{th}. All energy is to heat 18.61

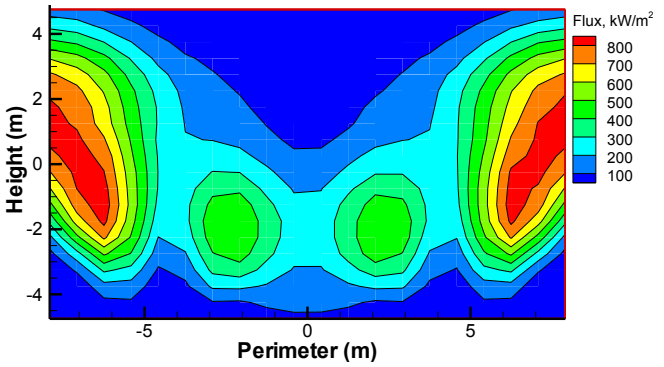

Fig. 4. Incident flux distribution for boiling receiver.

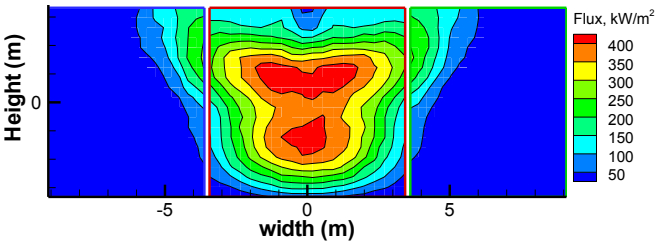

Fig. 5. Incident flux distribution for superheating receiver.

kg/s feedwater of 165 °C, 10.65 MPa to main steam of 513.5 °C, 10.12 MPa. Finally 25 % amount of steam is stored and supplies heat at the night, the remaining is used for 10 MW_e power station. The average steam quality at the boiler outlet is 6.67 %. Section 4 gives dryness for each panel.

3.3.1. Incident heat flux division and heat transfer fluid flow direction

The boiling tubes are all one-rising. As Fig. 4 shows, average flux on the cylinder is 253 KW/m^2. Along the perimeter, it comprises 18 panels. When calculating, every panel is divided into 12 sections along height. Maximum heat flux point value is 775 KW/m^2 and reduces a lot contrast to one aiming of 1280KW/m^2.The gross mass flow rate for all panels is 279.15 kg/s.

The flow layout for superheating cavity receiver inner walls is arranged according to the heat flux. As convective heat transfer coefficient in the superheating section is relatively low, flow velocity should be increased in the high heat flux parts. To solve this problem, panels on the back wall has less tubes to get higher velocity. As heat flux distribution on the inner walls is symmetrical, three walls are divided into two parts and each flows through

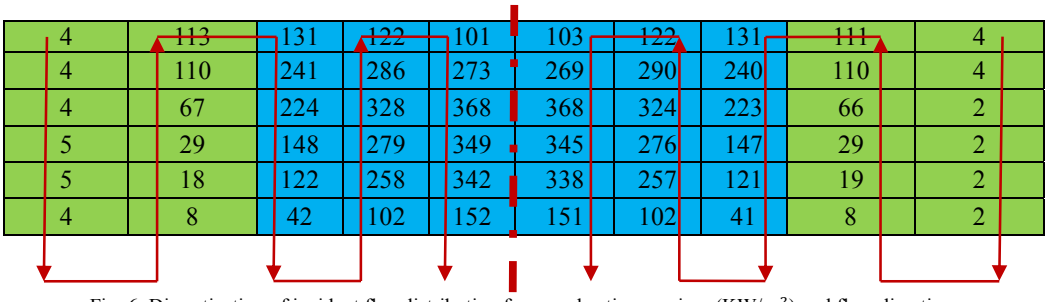

Fig. 6. Discretization of incident flux distribution for superheating receiver (KW/m²) and flow direction.

mass flow of 9.305 kg/s. The detailed flow direction for each panel is shown in Fig. 6, also incident heat flux division can be seen from this. Average heat flux for these three inner walls is 101 KW/m². And maximum heat flux value is 390 KW/m². It decreases much compares with only one aiming point of 880KW/m². Heat flux existing on the passive surfaces such as upper and bottom inner walls are respectively 21 KW/m² and 2 KW/m².

3.3.2. Heat loss

The main heat loss includes reflective loss, radiative loss and convective loss. Conductive loss is very small and can be ignored.

It is easy to obtain heat loss for boiler receiver in the case of obtaining the tube wall temperature. The calculations are as follows and the natural heat convection loss coefficient is evaluated by reference [6]:

$$Q_{B,ref,i} = A_{B,i} \cdot (1-a) \cdot q_{B,in,i} \tag{4}$$

$$Q_{B,rad,i} = A_{B,i} \cdot \sigma \cdot \varepsilon \cdot (T_{B,wall,i}^4 - T_\infty^4) \tag{5}$$

$$Q_{B,conv,i} = A_{B,i} \cdot h_{B,nc,i} \cdot (T_{B,wall,i} - T_\infty) \tag{6}$$

$$h_{B,nc,i} = 0.098 \cdot (\pi/2) \cdot Gr^{1/3} \cdot (T_{B,wall,i} / T_\infty)^{-0.14} \cdot \lambda / l \tag{7}$$

where $Q_{B,ref,i}$, $Q_{B,rad,i}$, $Q_{B,conv,i}$ are respectively reflective, radiative and convective loss for boiler panel i. a and ε are respectively absorptivity and emissivity of the tube walls, both equal 0.95. σ is Boltzmann constant. $q_{B,in,i}$ is the directly incident heat flux on the panel i. $h_{B,nc,i}$ is natural convective coefficient. $T_{B,wall,i}$ represents average wall temperature of panel i and T_∞ is the ambient temperature. $A_{B,i}$ is panel i area. Gr is the Grashof number.

For the superheating receiver, the calculation of heat loss through aperture is complex. The cavity includes 7 faces if assuming the entrance aperture as a face.

Reflective heat loss is solved similar to radiative heat loss calculation [7] as:

$$J_{S,ref,i} = (1-\varepsilon_i) \cdot q_{S,in,i} + (1-\varepsilon_i) \sum_{j=1}^{7} f_{i,j} J_{S,ref,j} \quad (i = 1,2,\ldots\ldots 7) \tag{8}$$

$$Q_{S,ref} = \sum_{i=1}^{7} A_{S,i} \cdot J_{S,ref,i} \cdot f_{i,7} \tag{9}$$

where $J_{S,ref,i}$ is the effective reflection leaving a surface including re-reflected fraction and direct reflection for the incident solar energy. For $i = 1,2,\ldots\ldots 6$, $\varepsilon_i = 0.95$, for $i = 7$, $\varepsilon_i = 1$. $A_{S,i}$ is area for each face. $f_{i,j}$ is view factor [8] between any two faces.

Radiative heat loss calculation [7] is shown as:

$$J_{S,rad,i} = \varepsilon_i \cdot \sigma \cdot T_{S,wall,i}^4 + (1-\varepsilon_i)\sum_{j=1}^{7} f_{i,j} J_{S,rad,j} \quad (i = 1,2,\ldots\ldots 7) \tag{10}$$

$$Q_{S,rad} = \sum_{i=1}^{7} A_{S,i} \cdot J_{S,rad,i} \cdot f_{i,7} \tag{11}$$

where $J_{S,rad,i}$ is the effective radiation leaving a surface including reflected fraction of the irradiation as well as direct emission.

Natural convective loss calculation adopts equations put forward by Siebers D.L [9]:

$$Q_{S,conv} = A_{S,7} \cdot h_{S,nc} \cdot (T_{S,wall,avg} - T_\infty) \tag{12}$$

$$h_{S,nc} = 0.81 \cdot (T_{S,wall,avg} - T_\infty)^{0.42} \tag{13}$$

where $A_{S,7}$ is the aperture area.

3.3.3. Heat transfer and flow calculation

To obtain temperature distribution on tube walls, a thermal efficiency assumption η should be given. Convection and conduction calculations for flowing in the tubes are as follows:

$$q_{i,,in} = q_{o,in} \cdot \eta \cdot d_o / d_i \tag{14}$$

$$T_{i,wall} = \frac{q_{i,in}}{\alpha_{foc}} + T_f \tag{15}$$

$$T_{o,wall} = \frac{q_{i,in} \cdot d_i \cdot Ln(\frac{d_o}{d_i})}{2 \cdot \lambda_{wall}} + T_{i,wall} \tag{16}$$

where η is an assuming thermal efficiency. $q_{o,in}$ is incident heat flux on the tube outer wall surface. $q_{i,in}$ is the heat flux on the inner tube wall. d_i , d_o are respectively inside and outside diameter of tube. α_{foc} is forced convection heat transfer coefficient. λ_{wall} is conductivity coefficient of tube wall. $T_{i,wall}$, $T_{o,wall}$ are separately temperature of inner and external tube wall. T_f is heat transfer fluid temperature.

Wall temperature is used for calculating heat loss, then a new thermal efficiency η' is generated. It compares with the previous one and does iteration.

The key problem is to determine α_{foc} for different flow patterns. For one-phase as water only or vapor only flowing in the tube [10], expression is listed as:

$$\alpha_{foc} = 0.023 \cdot \lambda_f \cdot \mathrm{Re}_f^{0.8} \cdot \mathrm{Pr}_f^{0.4} / d_i \tag{17}$$

where λ_f , Re_f , Pr_f are parameters of heat transfer fluid.

The start point and α_{foc} for subcooled boiling section are determined by [11]:

$$T_{wall} - T_f \geq \frac{4 \cdot \sigma \cdot T_{sl} \cdot v_{lh} \cdot \alpha_f}{\lambda_f \cdot h_{lh}} (1 + \sqrt{1 + \frac{\lambda_f \cdot h_{lh} \cdot (T_{sl} - T_f)}{2 \cdot \sigma \cdot T_{sl} \cdot v_{lh} \cdot \alpha_f}}) \tag{18}$$

$$\alpha_{foc} = \frac{\alpha_f}{2} (1 + \sqrt{1 + \frac{\lambda_f \cdot h_{lh} \cdot (T_{sl} - T_f)}{2 \cdot T_{sl} \cdot \sigma \cdot v_{lh} \cdot \alpha_f}}) \tag{19}$$

where α_f, λ_f, T_f are one-phase parameters. h_{lh}, v_{lh} are enthalpy and specific volume for latent heat. T_{sl} is saturated water temperature. σ is surface tension.

Saturated boiling zone is influenced by both macroscopic and microcosmic convection heat transfer [12], they can be calculated by:

$$\alpha_{foc} = \alpha_{foc,mac} + \alpha_{foc,mic} \tag{20}$$

$$\alpha_{foc,mac} = 0.023 \cdot \lambda_{sl} \cdot \mathrm{Re}_{tp}^{0.8} \cdot \mathrm{Pr}_{tp}^{0.4} \cdot F / d_i \tag{21}$$

$$\alpha_{foc,mic} = 0.00122 \cdot (\frac{\lambda_{sl}^{0.79} \cdot c_{sv}^{0.45} \cdot \rho_{sl}^{0.49}}{\sigma^{0.5} \cdot \mu_{sl}^{0.29} \cdot h_{lh}^{0.24} \cdot \rho_{sv}^{0.24}}) \tag{22}$$

where *sl* and *sv* separately represent saturated liquid and vapor parameters. *tp* is two-phase parameters. F is corrected coefficient.

For pressure drop calculation, both boiling and superheating receiver include frictional drag. As density of superheated steam is relatively low, weight loss can be ignored. But boiling section should consider it, as water accounts for a large proportion.

4. Results

Assuming mass flow rate in every panel is equal to 15.508 kg/s, and result shows that pressure drop differences for all panels are little. So this simplified method is permissible. As heat flux distribution on the boiling receiver is symmetrical along east and west direction, only half of the receiver surface as 9 panels need to be considered. Fig. 7 gives final wall temperature and heat transfer fluid outlet temperature. And the boundary between black and red

363.0 315.1	**355.5** 315.1	**342.4** 315.2	**332.7** 315.1	**324** 315.1	**322.3** 315.1	**320.7** 315.1	**318.9** 315.1	**317.1** 315.1
427.6 315.2	**410.2** 315.2	**386.8** 315.2	**360.3** 315.2	**340.0** 315.1	**332.4** 315.2	**327.9** 315.2	**323.1** 315.2	**319.2** 315.1
494.5 315.2	**470.8** 315.2	**433.3** 315.2	**393.7** 315.2	**358.0** 315.2	**343.8** 315.2	**336.2** 315.2	**328.2** 315.2	**321.6** 315.2
531.4 315.2	**507.4** 315.3	**462.4** 315.3	**413.1** 315.2	**372.2** 315.2	**354.2** 315.2	**344.8** 315.3	**333.7** 315.2	**324.8** 315.2
541.4 315.3	**523.2** 315.3	**478.8** 315.3	**420.9** 315.3	**356.2** 315.3	**361.7** 315.3	**356.1** 315.3	**342.1** 315.3	**330.5** 315.3
532.0 315.3	**545.0** 315.3	**505.3** 315.3	**425.0** 315.3	**356.7** 314.8	**373.1** 315.3	**373.4** 315.3	**357.1** 315.3	**333.2** 315.3
436.4 315.4	**543.5** 315.4	**523.5** 315.4	**430.8** 315.4	**356.3** 313.4	**392.5** 315.3	**404.5** 315.4	**381.2** 315.4	**343.5** 314.8
396.2 313.0	**460.3** 315.4	**533.1** 315.4	**390.7** 315.4	**354.6** 311.8	**380.1** 315.4	**437.8** 315.4	**376.3** 315.4	**353.0** 313.8
353.7 309.8	**416.3** 313.9	**447.5** 315.5	**374.9** 312.9	**345.3** 310.3	**379.0** 313.6	**404.0** 315.5	**378.8** 314.1	**356.0** 312.4
318.6 308.2	**357.6** 310.0	**392.2** 312.9	**355.0** 310.5	**330.1** 309.0	**364.6** 311.2	**384.4** 312.4	**365.7** 311.6	**348.3** 310.8
308.6 307.8	**317.9** 308.3	**345.5** 309.8	**328.1** 308.9	**316.1** 308.2	**339.2** 309.2	**351.6** 309.6	**344.0** 309.5	**336.6** 309.4
307.7 307.7	**312.5** 307.9	**329.0** 308.5	**320.5** 308.2	**312.5** 307.9	**318.4** 308.1	**316.8** 308.1	**322.2** 308.3	**326.5** 308.4

Fig. 7. Wall temperature (bold, top) and fluid outlet temperature (plain, bottom) of each element of the boiling receiver ($^{\circ}C$).

316.6 315.7	**370.6** 337.0	**374.2** 341.0	**465.6** 429.6	**464.4** 434.5	**463.3** 432.8	**463.9** 427.7	**373.0** 340.1	**369.1** 336.2	**316.5** 315.7
317.1 315.9	**361.0** 329.4	**411.0** 348.7	**507.3** 423.6	**529.6** 448.5	**526.6** 446.56	**506.7** 421.8	**409.4** 347.7	**360.1** 328.7	**316.9** 315.8
317.0 316.0	**341.2** 322.7	**415.7** 356.5	**504.6** 409.8	**578.4** 468.0	**576.1** 466.0	**501.5** 407.8	**414.3** 355.4	**340.5** 322.1	**316.5** 315.9
317.5 316.2	**326.9** 319.1	**401.8** 361.9	**474.1** 394.7	**592.1** 487.0	**588.5** 484.7	**471.2** 393.0	**400.1** 360.7	**326.4** 318.6	**316.4** 315.9
317.8 316.4	**322.7** 317.7	**399.7** 366.4	**454.5** 382.5	**609.1** 506.1	**605.4** 503.5	**452.7** 381.0	**398.1** 365.1	**322.3** 317.2	**316.4** 315.9
317.5 316.5	**319.0** 316.8	**379.4** 367.9	**400.1** 371.9	**560.3** 514.5	**557.6** 512.0	**398.7** 370.5	**378.0** 366.6	**318.5** 316.3	**316.6** 316.0

Fig. 8. Wall temperature (bold, top) and fluid outlet temperature (plain, bottom) of each element of the superheating receiver ($^{\circ}C$).

means starting point of generating vapor. At the exit, average dry vapor accounts for 6.67 % of total mass flow rate. And dryness for these 9 panels are respectively 12.4%, 15%, 14%, 6.6%, 2%, 3.5%, 4%, 2%, 0.5%. Maximum wall temperature reaches 545 $^{\circ}C$, no overheating will be occur. Pressure along panels drops from 10.65 MPa to 10.58 MPa. Total thermal efficiency of boiling receiver is 89.1 %. Reflective loss is 2100 KW, radiative loss is 1802 KW and convective loss is 672 KW. Reflective and radiative is relatively high.

As superheating receiver inner walls is divided into two parts, mass flow rate is 9.305 kg/s for both parts. Fig. 8 gives wall temperature and heat transfer fluid outlet temperature for cavity receiver. It comes to maximum wall temperature of 610 $^{\circ}C$, and maximum endurance of tube material is 850 $^{\circ}C$. Pressure drop is about 0.46 MPa. Because aperture area is small compares to the whole cavity structure, thermal efficiency is high of 96.47 %. Total

heat loss includes reflective loss 110 KW, radiative loss 309 KW and convective loss 92 KW. It is obvious that radiative loss is the main loss.

After overall calculation, dual-receiver presented in this paper has a thermal efficiency of 91 % and can be used to supply a 10 MW_e power plant.

5. Discussions and perspectives

A new concept for solar tower steam generation system design was presented and analyzed. As the heliostat field is divided into two parts respectively for boiling and superheating section, it is quick and simple to control the heat flux distribution on both section. Therefore, the arrangement of a dual-receiver separately for boiling and superheating section will be useful to short the start-up time. Adopting external absorber is beneficial for future increasing solar power plant capacity. And more uniform heat flux distribution obtained by multi-aiming strategy to avoid appearance of hot spot. For cavity receiver, layout of placing less tubes in the back wall panel than side wall panel is good for increasing convective heat transfer coefficient in the high heat flux parts.

Heliostats allocation for external and cavity receivers should be optimized for a higher heliostat field efficiency in the future work. Another study can be extension to transient analysis for the model to get how it works under different operation conditions. As main steam parameters play an important role in deciding cycle thermal efficiency of power plant, ultrasupercritical steam cycle power plants could be the next development step.

References

[1] Osuna R, Fernández V. 10 MW solar thermal power plant for southern Spain, report no. NNE5/1999/356. E-41018 Sevilla: Solúcar S.A., Avda. de la Buhaira 2; 2001.
[2] Gonzalez MS, Gonzalez-Aguilar RO. Solar concentration plant for the production of superheated steam. US 8,181,641 B2; 2012.
[3] Ben-Zvi R, Epstein M, Segal A. Simulation of an integrated steam generator for solar tower. Solar Energy; 2012, 86(1): 578-592.
[4] Siala FMF, Elayeb ME. Mathematical formulation of a graphical method for a non-blocking Heliostat field layout. Renewable Energy; 2001, 23: 77-92.
[5] Chunxu Du, Lijun Guo, Pu Wang. Introduction and application of SolTRACE. Solar Energy; 2011, 21: 17-21.
[6] Incropera F P, Lavine A S, DeWitt D P. Fundamentals of heat and mass transfer. John Wiley & Sons Incorporated, 2011.
[7] Montiel Gonzalez M, Hinojosa Palafox J, Estrada C A. Numerical study of heat transfer by natural convection and surface thermal radiation in an open cavity receiver. Solar Energy, 2012, 86(4): 1118-1128.
[8] Howell JR. <http://www.engr.uky.edu/rtl/Catalog/>, 11/8/11, University of Texas at Austin, Dep. of Mech. Eng;2010.
[9] Dennis L. Siebers, John S. Kraabel. Estimating convective energy losses from solar central receivers.Sandia Report (SAND84-8717), 1984.
[10] Shiming Yang, Wenquan Tao. Heat transfer theory. Beijing: People; 2006.
[11] Sato T, Matsumura H. On the conditions of incipient subcooled-boiling with forced convection. Bulletin of JSME; 1964, 7(26): 392-398.
[12] Zhonghu Lin. Two-phase of steam and water and heat transfer, first ed. Xian Jiaotong Uinversity Press; 1987.